Control of potential-wave profile in multiflow plasma systems

V. D. Fedorchenko, Yu. P. Mazalov, and A. S. Bakaĭ

Physicotechnical Institute, Academy of Sciences of the Ukrainian SSR, Kharkov
(Submitted 14 May 1978)
Zh. Eksp. Teor. Fiz. **76**, 107–120 (January 1979)

It is shown theoretically and experimentally that, by varying the beam-particle velocity distribution in a multiflow beam-plasma system, it is possible to control the distribution of trapped particles and hence the profile of the resulting wave. Two beams were injected into the plasma. One was used for the selective amplification of the wave (due to the post-critical value of its velocity) and the other was used to produce the necessary distribution function for the trapped particles and the initial perturbation. Particle trapping by the wave field and the subsequent evolution of the particle-wave system are examined. It is shown that sharp peaks or valleys in the potential are produced, depending on the relationship between the mean particle velocity and the initial phase velocity of the perturbation.

PACS numbers: 52.40.Mj

1. INTRODUCTION

Collisionless plasma has some remarkable properties. It can support the propagation of nonlinear waves of arbitrary profile, and the waves can be amplified with the aid of particle beams. The ability to produce waves with a required profile is of considerable interest both in physics and technology (it will be sufficient to mention the needs of accelerator technology and of electronics). However, the properties of collisionless plasma have not so far been fully exploited for these purposes because the control of evolutionary processes leading to the establishment of quasistationary nonlinear waves has not been adequately investigated.[1] In this paper, we show both theoretically and experimentally that a multiflow plasma system can be used to produce quasistationary nonlinear waves whose profile can be varied within very broad limits.

Nonlinear waves in collisionless plasma can be conventionally divided into two classes, depending on the nature of the interaction processes responsible for their appearance, namely, wave-wave and wave-particle processes. The former processes rely on the interaction between waves through nonresonance particles, whereas processes of the second type rely on the interaction between waves and resonance particles. The properties of nonlinear waves belonging to the first of these two classes were first investigated by Akhiezer and Lyubarskiĭ[1] (see also Refs. 2 and 3).

The wave-wave type nonlinear interaction is also basically responsible for solitary waves in bounded plasma when the initial disturbance is large enough, or in a bounded beam-plasma system when a periodic signal is applied to the input.[4-6] The interaction between waves and resonance particles leads to a change in its profile and its phase velocity. As far back as 1949, Bohm and Gross[7] found the correction to the dispersion relation due to trapped particles. The effect of the resonance-particle distribution on the dispersion of waves was first demonstrated experimentally by Fedorchenko et al.[8]

Nonlinear waves due to a special distribution of res-onance particles were described by Bernstein et al.[9] and have since been referred to as BGK waves. It has been shown[9] that, by specifying a particular distribution function for the trapped electrons and ions, it is possible to ensure that the stationary wave assumes the required profile. It has not so far been possible to produce BGK waves of a required profile because evolutionary processes have not as yet been adequately investigated.

Bakaĭ[10,11] has developed a self-consistent theory of slowly evolving BGK waves,[2] which can be used as a basis for establishing the necessary initial homogeneous particle distribution function which will ensure that the BGK wave will have a prescribed profile.

Two limitations were established as a result: (a) the profile of the slowly evolving wave is symmetric relative to the extremal points when resonance particles of only one type are present, and (b) the number of extremal points on the wave profile remains constant throughout the slow evolution process. Moreover, the wave profile is more sensitive to changes in the distribution of trapped particles for small wave amplitudes, so that the initial stage of the evolution of the wave is more favorable for changes in its shape.

In beam-plasma systems in which beam instability develops, the initial stage cannot be described within the framework of the theory of slowly evolving waves, but the results of this theory are still useful for the qualitative examination of the process. There is also a series of numerical experiments in which the formation of the BGK waves was investigated as a result of the development of beam instability (see, for example, the paper by Astrelin et al.[12] and the bibliography therein). The results of these experiments can be used to throw some light on the evolution of the distribution function of the resonance particles.

We have used the foregoing ideas as a basis for our study of the evolution of waves in a bounded plasma column, located in a strong magnetic field, into which two electron beams are injected. The density of the first (main) beam, n_1, is comparable with the plasma

density, and the beam is used mainly to amplify the waves. The density of the second (controlling) beam, n_2, is much less than the plasma density, and the beam is used to control the wave profile. Apart from the choice of the initial distribution in the controlling beam, we must also specify the velocity of the main beam. The point is that, usually, the dispersion properties of the beam-plasma system ensure the amplification of a broad wave spectrum. This results in a distortion of the evolutionary process in which we are interested and, to avoid it, we must produce selective amplification of the waves formed by the controlling beam. A suitable method for doing this is to use beams with post-critical velocity in a bounded plasma. This method has been investigated both theoretically[10,11] and experimentally.[13-15] The presence of this type of beam ensures the amplification of only those waves whose amplitude exceeds a certain critical value. Low-amplitude noise is, therefore, not amplified by the post-critical beam, and does not produce additional interference in the system.

Providing the above conditions are satisfied, it is possible to produce nonlinear waves whose profile can be controlled within broad limits with practically no effect on the average plasma parameters.

2. THEORETICAL ANALYSIS

We shall show that a two-beam plasma system with slightly post-critical main beam can be used to produce quasi-stationary BGK waves with a controllable profile.

Let us begin by considering the conditions for the amplification of finite-amplitude waves in such a system. Consider a bounded plasma column in a strong magnetic field ($\omega_H \gg \omega_p$, where ω_H and ω_p are the electron-cyclotron and electron-plasma frequencies) into which two beams are injected, namely, the main beam and the controlling beam with densities $n_1 \approx n_0$ and $n_2 \ll n_0$, respectively. The dispersion of the waves in which we are interested is determined both by the beam and by the plasma. Because of magnetization, the motion of the electrons is one-dimensional, and the dispersion relation for the potential waves is[16]

$$\frac{\omega_1^2}{(\omega - k_\parallel v_1)^2} + \frac{\omega_p^2}{\omega^2} = 1 + \frac{k_\perp^2}{k_\parallel^2}, \tag{1}$$

where $k_\parallel$ and $k_\perp$ are the longitudinal and transverse components of the wave vector, respectively, v_1 is the velocity of the main beam, and

$$\omega_1^2 = 4\pi n_1 e^2/m, \quad \omega_p^2 = 4\pi n_0 e^2/m.$$

Equation (1) has the following solution when $\omega_1 = \omega_p$:

$$\left(\omega - k_\parallel \frac{v_1}{2}\right)^2 = \frac{k_\parallel^2 v_1^2}{4} + \frac{\omega_p^2 k_\parallel^2}{k_\perp^2 + k_\parallel^2} \pm \left[\frac{\omega_p^2 k_\parallel^4 v_1^2}{k_\perp^2 + k_\parallel^2} + \frac{\omega_p^4 k_\parallel^4}{(k_\perp^2 + k_\parallel^2)^2}\right]^{1/2}. \tag{2}$$

From this, it is clear that when

$$\sigma^2 = k_\perp^2 v_1^2/\omega_p^2 < 8$$

we have an unstable branch of the oscillations (Fig. 1a) such that

$$\text{Re } \omega = k_\parallel v_1/2, \quad \text{Im } \omega > 0 \tag{3}$$

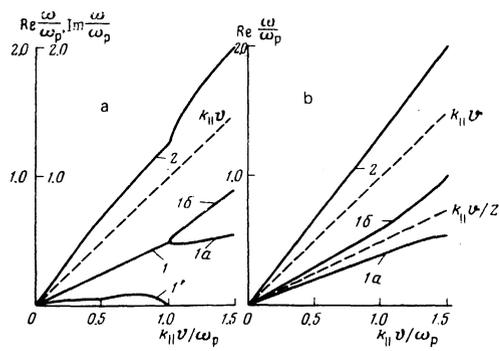for $k_\parallel < k_{\text{crit}} = [8\omega_p^2/v_1^2 - k_\perp^2]^{1/2}$.

FIG. 1. Dispersion curves for the beam-plasma system when the densities are equal: (a) curve 1—$\text{Re}(\omega/\omega_p)$, 1'—$\text{Im}(\omega/\omega_p)$, 2—constant intensity wave; $\sigma^2 = k_\perp v/\omega_p)^2 = 7.0$. (b) Curves 1a and 1b—$\text{Re}(\omega/\omega_p)$, 2—constant intensity wave; $\sigma^2 = 8.0$, Im $(\omega/\omega_p) = 0$.

When $\sigma^2 \geq 8$, the unstable branch vanishes [it is clear from (3) that $k_{\text{crit}} \to 0$ as $\sigma^2 \to 8$] and, consequently, finite-amplitude waves are stable in the system. The dispersion curves corresponding to $\sigma^2 = 8$ are shown in Fig. 1b.

We are interested in the conditions necessary for the amplification of the wave when $\sigma^2 \geq 8$. This condition was obtained by Bakaĭ[10] for $n_1 \ll n_0$ and was subsequently confirmed experimentally.[13] The amplified wave is an electron plasma wave with a dispersion relation determined by the plasma electrons, distortion by the beam being negligible.

On the other hand, when $n_1 \approx n_0$, this approximation is no longer valid. The instability of a finite-amplitude wave is then found to appear, just as in the case of a weak beam, because there is a change in the velocity of the particles interacting with the wave. Particles with velocities lower than the critical velocity appear when the wave amplitude is large enough, and this leads to the development of instability. The change in the velocity of particles moving in the field of the potential wave can easily be estimated from the conservation of the particle energy if we neglect the change in the wave amplitude during one particle-oscillation period:

$$m(v - v_{\text{ph}})^2/2 - e\varphi_0 \sin k\xi = W = \text{const}, \tag{4}$$

where $\xi = x - v_{\text{ph}}t$ is the position coordinate in the frame in which the wave with phase velocity v_{ph} and amplitude φ_0 is at rest. The change in the beam velocity can now be estimated from (4):

$$\Delta v = 2e\varphi_0/m(v_1 - v_{\text{ph}}). \tag{5}$$

This expression describes the change in the velocity of transmitted particles for which $v_1 - v_{\text{ph}} \gg \Delta v$. In the case in which we are interested [see (3)], we have $v_1 - v_{\text{ph}} \approx v_1/2$ and the last inequality is satisfied for amplitudes that are not very large.

To obtain the criterion and growth rate for the instability of finite-amplitude waves, we must replace v_1 in (2) with $\bar{v}_1 = v_1 - \alpha\Delta v$, i.e., the velocity of the beam less the reduction in the velocity of the particles during the interaction with the wave. The quantity α is a numerical parameter of the order of unity, which

represents the fact that the beam ceases to be mono-chromatic as a result of the interaction with the wave. We may assume that $\alpha = 1$ for the estimates to which we shall confine our attention here. The final result is, therefore, the following nonlinear dispersion relation for finite amplitude waves:

$$\left(\omega - k_{\parallel}\frac{\tilde{v}_1}{2}\right)^2 = \frac{k_{\parallel}^2\tilde{v}_1^2}{4} + \frac{\omega_p^2 k_{\parallel}^2}{k_{\perp}^2 + k_{\parallel}^2}$$
$$\pm \left[\frac{\omega_p^2 k_{\parallel}^4\tilde{v}_1^2}{k_{\perp}^2 + k_{\parallel}^2} + \frac{\omega_p^4 k_{\parallel}^4}{(k_{\perp}^2 + k_{\parallel}^2)^2}\right]^{1/2}, \quad (6)$$
$$\tilde{v}_1 = v_1 - 2e\varphi_0/m(v_1 - v_{ph}).$$

It follows from this equation that the wave belonging to branch 1 (see Fig. 1b) is stable for an infinitely small amplitude, but becomes unstable as soon as

$$v_1 - 2e\varphi_0/m(v_1 - v_{ph}) < v_{crit},$$
$$v_{crit} = 2\sqrt{2}\omega_p/(k_{\parallel}^2 + k_{\perp}^2)^{1/2},$$

or

$$\varphi_0 > \varphi_{crit} = m(v_1 - v_{ph})(v_1 - v_{crit})/2e. \quad (7)$$

This inequality is the condition for the amplification of a finite-amplitude wave in the beam-plasma system on the assumption that the beam and plasma densities are equal.

Next, we consider the possible control of the wave profile through the use of resonance particles. Resonance particles are defined as particles whose total energy W in the system in which the waves are at rest does not exceed $1.1e\varphi_0$. The equation describing the profile of a stationary wave in this system is

$$d^2\varphi/d\xi^2 + 4\pi e\rho(\varphi) = 0. \quad (8)$$

The expression for the charge density $\rho(\varphi)$ includes contributions of both resonance and nonresonance particles, so that $\rho(\varphi)$ can be written in the form

$$4\pi e\rho(\varphi) = k_{\parallel}^2\varphi + 4\pi e\rho_1(k, \varphi), \quad (9)$$

where $\rho_1(k, \varphi)$ is the charge density due to the trapped particles. Given the wave profile $\varphi(\xi)$, we obtain the following expression for $\rho_1(k, \varphi)$ from (8) and (9):

$$4\pi e\rho_1(k, \varphi) = -\varphi''(\xi) - k_{\parallel}^2\varphi(\xi), \quad (10)$$

which determines the distribution function $f_1(\xi, v)$ for the trapped particles:[9]

$$f_1(\xi, v) = f_1(W) = \frac{\sqrt{2m}}{\pi}\int_{e\varphi_{min}}^{-W} du \frac{d\rho_1(u)}{du}[-W-u]^{-1/2}, \quad (11)$$

$$W = \frac{mv^2}{2} - e\varphi, \quad \varphi_{min} = \min\varphi(\xi), \quad W < -e\varphi_{min}.$$

We note that the choice of the profile $\varphi(\xi)$ is not entirely arbitrary because the distribution function u must be nonnegative and the function itself must be symmetric relative to the external points when trapped particles carrying charges of a particular sign are present.[10,11]

We are interested in BGK profiles in the form of narrow peaks and valleys in the potential because the excitation of such waves is of considerable practical importance and has been the main target of experimental studies. It is not difficult to indicate the trapped-electron distribution necessary for such waves without going into a detailed analysis of (10) and (11). Since $\rho_1(v) > 0$, an addition to the number of trapped electrons
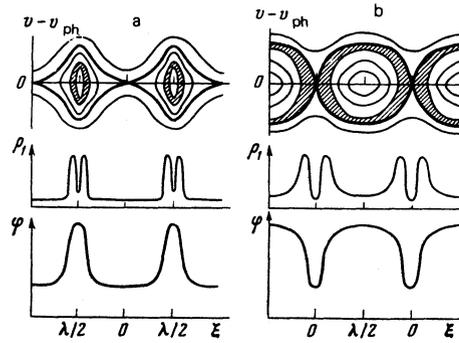

FIG. 2. Distribution of trapped electrons on the phase plane, their charge densities, and the wave profiles corresponding to the distributions.

will result in a reduction in the second derivative $\varphi''(\xi)$. It follows that if the trapped electrons are localized near the potential maximum, i.e., in the neighborhood of the bottom of the potential well for the electrons, the result is the appearance of sharp potential peaks. Figure 2a shows the distribution of the trapped electrons (shaded region on the phase plane) and their charge density, together with the profile of the wave corresponding to this case.

If, on the other hand, the trapped electrons are localized near the minima of $\varphi(\xi)$, this will flatten the potential in the region of the maxima and will result in the appearance of a wave profile in the form of sharp potential valleys. The wave profile, the particle distribution, and the charge distribution in this case are shown in Fig. 2b.

The foregoing discussion leads to the following scheme for the excitation of a wave with a controllable profile. A priming wave with amplitude exceeding the critical value given by (7) is produced in a system with a slightly post-critical main beam, and this leads to the selective amplification of this wave in the system. The controlling beam, whose initial distribution function can be varied to ensure the required trapped-particle distribution, is injected in order to control the profile of this wave (see Fig. 2).

It is important to note that, whilst the above analysis demonstrates the nature of the trapped-electron distribution that will result in the required profile of the quasistationary potential wave, it does not concern itself with the evolution of the wave or the distribution function of the resonance particles during the initial stage of development of the beam instability. So long as the wave amplitude is small, and the trapped particles do not succeed in executing many oscillations in the wave field, the evolutionary process is not adiabatic during this stage, and the results of the theory of slowly evolving waves[10,11] can only be used as an indication of how the initial distribution function should be chosen for the controlling beam in order to ensure that the required results will be achieved.

The evolution of the distribution function of the trapped particles in the system under investigation are discussed further in Sec. 4 together with the experimental results.

Finally, we note that the selective amplification of a large-amplitude wave by a beam with initial velocity exceeding the critical value does not completely exclude the possibility that noise waves resulting from the interaction between the beam particles and the large-amplitude waves will take place. However, the characteristic time for the interaction between the beam particles and the wave is inversely proportional to the square root of the wave amplitude, and is much smaller than the characteristic time for the interaction between the particles and the noise waves, so that the coherence of the interaction between the beam particles and the noise waves is violated during the initial stage, and the growth of the noise waves is unimportant. Other waves can also be excited during the stage corresponding to the saturation of the large-amplitude wave to which the beam has transferred most of its energy. For example, the development of modulation instability involving the trapped particles may have this effect, but this process is slow and is not experimentally well defined (see Sec. 3 and Ref. 17).

3. EXPERIMENTS

The experiments were performed with a two-beam system in which the density of the main beam and of the plasma in the strong magnetic field were equal ($\omega_H \gg \omega_{pe}$). The frequency of the waves was much smaller than the electron plasma frequency of the system. The velocity v_1 of the main electron beam was chosen to be close to the critical velocity v_{crit} for which the beam-plasma system was stable. The current in the second, controlling, electron beam was much smaller than the current in the main beam.

The system is illustrated schematically in Fig. 3. Hollow electron beams (diameters 1 and 0.25 cm, respectively) are allowed to pass through a metal tube, 9 cm in diameter, placed in a uniform magnetic field of 800 Oe. The electrons are injected by the guns 2 and 3. The electron emitter is a tungsten wire, 0.05 cm thick. The energy of the external (main) beam is in the range 200–300 V, which corresponds to the velocities in the range $0.85 \times 10^9 - 1.04 \times 10^9$ cm/sec. The current in the main beam is held at 10 mA. The mean energy of the controlling beam varies from 40 to 300 V, with the current held at not more than 10% of the current in the main beam. The plasma is produced by ionization of the residual gas by the electron beam at a working pressure of 2×10^{-6} Torr in the chamber.

When the velocity of the main beam is equal to or greater than 8.5×10^8 cm/sec, the system is stable against natural electron-plasma oscillations, but, as the beam velocity is reduced, the beam-plasma instability is found to develop in the system. It follows that $v_{crit} = 8.5 \times 10^8$ cm/sec under the above experimental conditions.

The velocity of the perturbation in the subcritical state is equal to half the velocity of the main beam, which indicates that the beam and plasma densities are equal [see (3)]. Independent determination of the shift of the resonance frequency of the hollow cavity resonator due to the presence of the beam and plasma
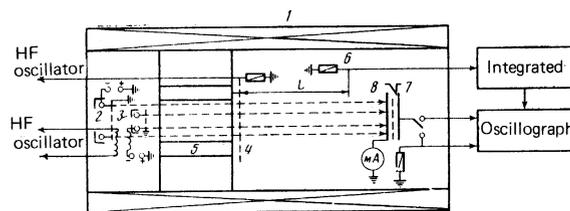

FIG. 3. Schematic illustration of the experimental system: 1—solenoid; 2, 3—electron guns; 4—feeding electrode; 5—bunching channel; 6—mobile probe; 7—collector of the electrostatic analyzer; 8—collector.

was performed by a method analogous to that used by Fedorchenko et al.[18] and confirmed that the two densities were, in fact, equal. Once we knew the parameters of the beam and its geometry, we could easily estimate that, in this case, $n_1 = n_0 = 5 \times 10^8$ cm^{-3}. The geometry of the electron beam was investigated along the length of the system with the aid of a mobile fluorescing screen. It was found that the cross section of the electron beam in the interaction region in the above magnetic field corresponded to the size of the cathode and that, since the Larmor radius of the plasma electrons was small (~ 0.01 cm), the regions occupied by the plasma electrons and by the main beam coincided.

The initial perturbation in the system is produced in one of two ways, namely, by bunching the controlling electron beam or by supplying a sinusoidal voltage to the priming electrode 4 which was in the form of a tungsten grid with 95% transmission and 3 cm diameter. Beam bunching was produced by modulating the accelerating potential on the electron gun 3, which was operated under saturation conditions. The modulation was established by applying the output of a ~10-MHz oscillator to a transformer connected to the gun cathode. The electron bunching occurs in the channel 5 (channel length 50 cm). The shape and velocity of the oscillations were investigated with the aid of a mobile probe 6 in the form of an antenna made from a tungsten wire (0.02 cm in diameter) loaded with a resistance equal to the wave impedance of the cable. The probe was capacitively coupled to the oscillations
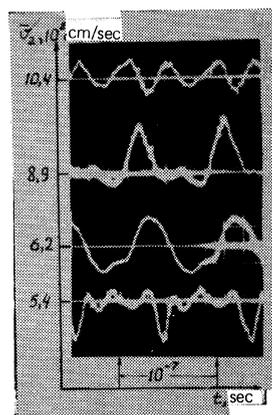

FIG. 4. Oscillations in the circuit of the mobile probe as functions of the mean velocity of the additional $\bar{v}_2$; $v_1 = 1.04 \times 10^9$ cm/sec, $f = 11.8$ MHz, $L = 60$ cm.
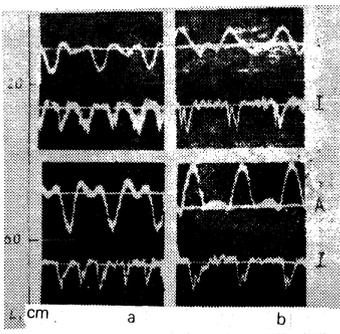
FIG. 5. Evolution of potential pulses (velocities are in cm/sec): (a) $v_1 = 1.04 \times 10^9$, $\bar{v}_2 = 5.4 \times 10^8$, $f = 11.8$ MHz; (b) $v_1 = 1.04 \times 10^9$, $\bar{v}_2 = 8.9 \times 10^8$; $f = 11.8$ MHz.

under investigation, and the rate of variation of the potential was recorded for the above frequencies. After passing through a wide-band amplifier, the probe signal was integrated and fed to an oscillograph. The electrostatic analyzer 7 was then used to determine the energy characteristics of both the main and controlling beams. When the initial perturbation was produced by the bunched beam, the shape of the recorded oscillations was found to be very dependent on the mean velocity $\bar{v}_2$ of this beam (Fig. 4). It was nonsinusoidal and, for certain values of $\bar{v}_2$, took the form of unipolar pulses. We have investigated the conditions necessary for the appearance of such waveforms and their evolution.

Figures 5a and b illustrate the dynamics of the production of the positive and negative potential pulses along the wall of the system. When the velocity of the main beam is somewhat higher than the critical value ($v_1 = 1.04 \times 10^9$ cm/sec) and the mean velocity of the bunched beam is $\bar{v}_2 = 5.4 \times 10^8$ cm/sec, a sequence of negative potential pulses is produced at the end of the system (Fig. 5a). An increase in the mean velocity of the additional beam is eventually accompanied by a change in the sign of the observed pluses (Fig. 5b). Analysis of oscillograms of this kind can be used to construct the dependence of the amplitude and velocity of the waves on the distance L (Fig. 6). As the unipolar pulses evolve, there is an increase in their
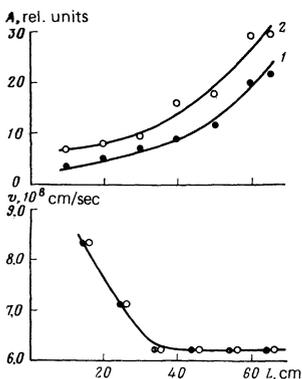
amplitude and a reduction in their velocity. We note that a negative pulse is produced when the mean velocity of the bunched particles in the controlling beam at the beginning of the system is less than the phase velocity of the wave excited by it. If, on the other hand, the velocity at the beginning of the system is of the order of the phase velocity of the perturbation, unipolar positive potential pulses propagate through the plasma. This picture changes when the velocity of the main beam becomes much greater than the critical value ($v_1 \gg v_{crit}$). The initial perturbation is then found to decay gradually toward the end of the system.

To establish the mechanism responsible for the appearance of the above waves, we investigated the variable component of the electron-beam current. This was done by receiving part of the electron current on the analyzer collector (Fig. 3) from which the variable component of the current developed across a resistance equal to the wave impedance of the cable was fed into a wide-band amplifier and then into an oscillograph. The position of this component relative to the potential pulses along the system was determined. At each point in space, we first recorded the potential pulses with the probe 6 and then placed the analyzer-collector 7 at the same point. The shape of the recorded potential pulses was not found to depend on the position of the collector 7 relative to the probe 6, since there was no reflected signal in the two-stream system because one of the streams was lost to the collector.

Figures 7a and b show oscillograms of the potential pulses and of the variable component of the current for different values of $\bar{v}_2$ at the beginning and end of the plasma column. It is clear that, when the observed pulses are not unipolar, the appearance of the variable component of the current is different. When the waveform is entirely positive, each potential peak corresponds to a complicated current pulse, the position of which coincides with the potential maximum along the entire length of the plasma column. The negative potential corresponds to two current pulses located on either side of the potential minimum. This behavior of the variable component of the current indicates that it is due to the presence of particles with mean velocity
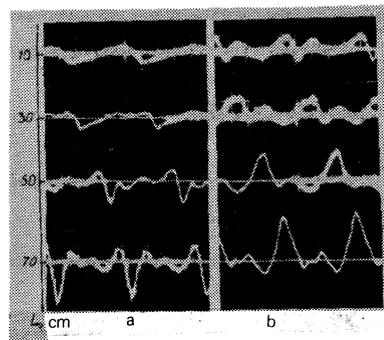

FIG. 6. Amplitude A and velocity v of BGK waves as functions of distance L: (1) $\bar{v}_2 = 5.4 \times 10^8$ cm/sec, (2) $\bar{v}_2 = 8.9 \times 10^8$ cm/sec.

FIG. 7. Oscillations in the circuit of the mobile probe (A) and the analyzer-collector (I) for different mean velocities of the additional beam. Oscillogram A represents the variation in the electric field in the plasma, whilst oscillogram I represents the variation in the current: (a) $\bar{v}_2 = 5.4 \times 10^8$ cm/sec, (b) $\bar{v}_2 = 8.9 \times 10^8$ cm/sec.
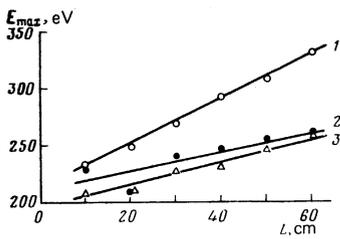
FIG. 8. Maximum energy of trapped particles as a function of distance L: 1—left-hand current peak; 2—right-hand current peak, both for $\bar{v}_2 = 5.4 \times 10^8$ cm/sec; 3—$\bar{v}_2 = 8.9 \times 10^8$ cm/sec.

equal to the phase velocity of the potential perturbation, and that their position relative to this perturbation determines its sign.

The analyzer 7 (Fig. 3) was used to determine the maximum energy of particles in the observed current pulses and its variation along the length of the system, both in the case of positive and negative formations. The results are shown in Fig. 8. It is noticeable that the maximum energies corresponding to potential minima on the left and right of the current peaks are different.

The analyzer was also used to investigate the energy composition of the main beam at exit from the system. In the absence of the controlling beam, the energy spread of electrons in the main beam was small, indicating that the beam-plasma system was stable. When the bunched controlling beam was injected, a wave was excited in the system and an energy spread among the main beam electrons was observed. At the same time, the maximum of the distribution shifted toward lower energies. The total energy lost by the main beam was about 15%. The main beam was thus found to transfer its energy to the wave if the initial amplitude were large enough and both particle bunching in the additional beam and the particles of the main beam participated in the generation of the potential waves.

When the perturbation in the system was produced by the second method (by supplying the sinusoidal potential difference derived from an external source to the feeder electrode), the behavior of this perturbation was investigated as a function of its initial amplitude and the velocity of the main and controlling beams (the latter was not modulated in this case because the
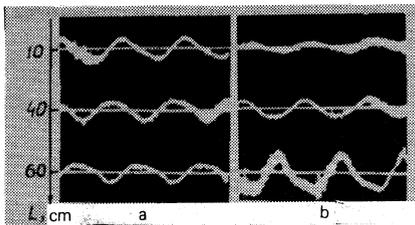

FIG. 9. Evolution of initial perturbation in the absence of the additional beam ($v_2 = 0$) for different velocities of the main beam: (a) $v_1 = 1.04 \times 10^9$ cm/sec, $f = 12.8$ MHz, $\tilde{U} = 12$ V: (b) $v_1 = 8.3 \times 10^8$ cm/sec, $f = 12.8$ MHz, $\tilde{U} = 3$ V.
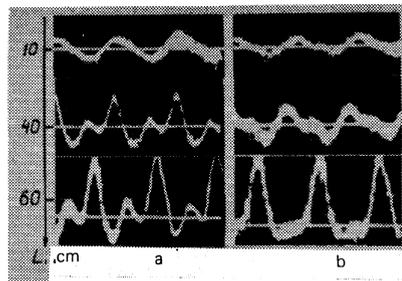

FIG. 10. Evolution of initial perturbation in the presence and absence of the additional beam: (a) $v_1 = 1.04 \times 10^9$ $v_2 = 0.63 \times 10^9$; (b) $v_1 = 8.3 \times 10^9$, $v_2 = 0$: in both cases, $f = 12.8$ MHz, $\tilde{U} = 12$ V (velocities in cm/sec).

time taken by the particles of this beam to traverse the region of variation in the potential in the region of the priming electrode was much shorter than the oscillation period).

In the absence of the additional beam, and when the velocity of the main beam is in excess of the critical value, the signal propagates without amplification at constant velocity (6×10^8 cm/sec, Fig. 9a). When the velocity of the main beam is reduced to 8.3×10^8 cm/sec, the system becomes unstable and the shape of the observed oscillations is very dependent on the amplitude of the initial perturbation. When the initial perturbation is small (Fig. 9b), unipolar pulses are not produced, the initial signal is amplified, and its velocity is equal to half the beam velocity. An increase in the amplitude of the initial perturbation by a factor of 4 (Fig. 10b) results in the appearance of positive potential pulses at the end of the system.

By injecting the additional beam with velocity in excess of the phase velocity of the perturbation, it is also possible to produce unipolar positive pulses which propagate at constant velocity (4×10^8 cm/sec, Fig. 10a). A reduction in the velocity of the additional beam does not lead to the appearance of negative pulses in this case. The initial perturbation gradually decays toward the end of the system.

4. DISCUSSION

We must now analyze the experimental data and compare them with theoretical predictions.

We shall consider the evolution of BGK waves when the perturbation is defined by a bunched controlling beam. It is clear from Fig. 6b that the velocity of the perturbation produced at the beginning of the system is very different from half the velocity of the main beam. This indicates that the system is stable and that the initial perturbation velocity v_{phi} is determined by the corresponding dispersion relation (curve 1b in Fig. 1b) and is independent of the mean velocity of the bunched beam. This is then followed by a rapid reduction in the phase velocity of the wave down to a value close to $v_1/2$. The time taken for this to happen is about 4×10^{-8} sec, which is much less than the period of the excited oscillations ($T \sim 10^{-7}$ sec). Amplification of the initial perturbation is observed at the

same time (Fig. 6a). The system has thus become unstable and the velocity of the amplified signal, v_{ph}, is now determined by a different dispersion relation (curve 1, Fig. 1a). Theoretical analysis indicates that this transition is due to the presence of the finite-amplitude wave and, according to (7), its amplitude in our case should be not less that 12 V ($v_1 = 1.04 \times 10^9$ cm/sec, $v_{crit} = 8.5 \times 10^8$ cm/sec, and $v_{ph1} = 8.3 \times 10^8$ cm/sec). We can now estimate the amplitude of the potential perturbation introduced by the bunched beam by substituting the charge distribution in the beam into the Poisson equation (by analogy with the procedure used by Fedorchenko et al.[6]). When the current in the additional beam is $i_1 = 1$ mA, the mean energy is $\overline{U}_2 = 220$ eV, the modulating voltage is $\tilde{U} = 25$ V, and the modulation frequency is $f = 12$ MHz, the amplitude of the plasma wave excited by a bunch may reach 20–25 V at the point where the electron trajectories begin to cross (in our case, this is the point at which the bunch enters the plasma, $L = 0$).

As noted above, the shape of the observed oscillations depends on the relation between the mean velocity of the additional beam and the phase velocity of the initial perturbation. This can be explained as follows. When the initial phase velocity of the perturbation and the mean velocity of the bunched particles are close to one another, the trapping of the bunched particles by the field of the initial perturbation occurs at relatively small amplitudes. Under the above experimental conditions, the phase velocity of the perturbation at the beginning of the system is 8.3×10^8 cm/sec and the mean velocity of the bunch particles is 8.9×10^8 cm/sec. When the modulation amplitude is $\tilde{U} = 25$ eV, the bunch contains particles with velocities in the range $8.3 \times 10^8 - 9.3 \times 10^8$ cm/sec, i.e., they are all greater than the phase velocity of the wave and are concentrated in a small phase volume, which corresponds to the trapped electrons being localized in the upper part of the phase plane shown in Fig. 2a. It is easily estimated that an amplitude of 3 V is sufficient to trap the most energetic electrons in this beam. Since the initial perturbation amplitude is substantially higher, the electrons are concentrated in the neighborhood of the bottom of the potential well, i.e., near the maximum of the potential. This is followed by a fast (in a time of about 4×10^{-8} sec) reduction in the phase velocity of the perturbation, connected with the transition of the system from the post-critical state to the instability region. The velocity falls from 8.3×10^8 to 6.2×10^8 cm/sec and, as a result, the trapped particles assume a retarding phase, begin to give up their energy to the wave, and remain near the bottom of the potential well during the slowing-down process. This is precisely the reason why the measured position of the variable component of the current in Fig. 7 coincides with the maximum of the potential throughout the length over which the interaction takes place. All this is accompanied by an increase in the perturbation amplitude (curve 2, Fig. 6a): after the point at which the phase velocity becomes stabilized, the amplitude increases by a factor of 3 in a time of 10^{-7} sec. The trapped particles then execute phase

oscillations relative to the wave with frequency $\Omega = k(e\varphi/m)^{1/2}$, and the inner part of the phase region containing the trapped particles for the amplitudes reached after the 10^{-7} sec assumes the form shown in Fig. 2a as a result of rotation because a proportion of the trapped particles will move downward from the upper part of the phase plane during the half-period. The result of all these processes is the formation of the sharp potential peaks observed in the experiment (Fig. 5b). The fact that this process does, in fact, proceed in this way is evidenced by the measured dependence of the maximum energy of particles corresponding to the variable component of the current on the length of the system (curve 3, Fig. 8). When the mean phase velocity of the formation is $v_{ph} = 6.2 \times 10^8$ cm/sec, the current peak at the end of the system includes particles with maximum energies of 250 eV. If we suppose that the amplitude reached by this time is responsible for the maximum energy of these particles, i.e.,

$$E_{max} = \tfrac{1}{2}m[v_{ph} + 2(e\varphi/m)^{1/2}]^2,$$

we find that the necessary value of this amplitude is about 40 V. This amplitude level is, in fact, reached at the end of the system because we estimate φ_{crit} to be ~12 V and an increase in the signal amplitude by a factor of three by the time the end of the system is reached is, in fact, confirmed experimentally (Fig. 6a).

Potential valleys similar to those shown in Fig. 2b were observed (Fig. 5a) when the mean velocity of bunch particles was much less than the initial phase velocity of the perturbation which, as in the above case, was equal to 8.3×10^8 cm/sec and was determined by the same dispersion law. For the same modulation amplitudes, the bunch contains electrons with velocities in the range $4.5 \times 10^8 - 6.2 \times 10^8$ cm/sec. It is clear from Fig. 6b that, as in the previous case, and for the same reasons, there is a reduction in the phase velocity but, in contrast to the situation examined above, only the most energetic electrons present in the distribution can be trapped at the beginning of the system for the above amplitude levels. Moreover, they immediately enter the accelerating phase, load the wave, and are concentrated near the "apex" of the potential energy $e\varphi$ at the time when the phase velocity of the perturbation becomes stabilized (Fig. 2b). The region near each such "apex" is also found to contain electrons with lower energies, which can now be trapped by the wave because the phase velocity of the perturbation has fallen. The electrons trapped near $\xi = 0$ can remain in the region of the potential minimum (i.e., near each "apex" of the potential energy) for a long time because the electron oscillation frequency in the field of the wave becomes zero on the separatrix dividing the trapped particles from those passing through (thick line in Fig. 2b). Since, as the potential valleys are being formed, the fast electrons that were trapped at the initial instants of time are still experiencing acceleration by the wave field, some of them may "roll over" the potential-energy "apex" and thus determine the character of the energy distribution of the trapped particles in each of the peaks of the charge distribution $\rho_1(\xi)$ shown in Fig. 2b. It is clear that

particles in the left-hand peak of this distribution should have the maximum energy. This is confirmed experimentally. In fact, we see from curves 1 and 2 of Fig. 8 that the maximum energies corresponding to the left- and right-hand current peaks are different.

We have also established experimentally that BGK waves appear even when an unbunched controlling beam, which defines the initial perturbation, is injected into the system (Fig. 10a). Such waves are only produced when the velocity of the controlling beam is greater than the phase velocity of the initial perturbation. The wave formation process is now again connected with the transition of the system from a stable to an unstable state. This is indicated by the growth in amplitude with distance, and the difference between the velocity of these waves and the velocity of the initial perturbation. The nonlinear waves are then formed more slowly, and the evolution terminates only at the end of the system. This is connected with the fact that the necessary distribution of trapped particles is established only by the phase oscillations in the field of the perturbation, and the time spent in this process is, of course, much greater than the time necessary for the analogous oscillation waveform to develop in the case of a bunched controlling beam. The fact that negative pulses cannot be produced in this case is explained by the fact that, when the velocity of the controlling beam is reduced, the beam enters the accelerating phase of the wave field, and this leads to its attenuation.[17,19] The formation of unipolar pulses when the amplitudes of the initial perturbation are substantially increased (in the absence of the controlling beam and in the presence of developed instability) is shown by estimates to be due to the trapping of particles from the main beam.

---

[1] Stationary nonlinear waves in collisionless plasma are usually unstable, but the decay time of such waves may be much longer than the characteristic time for their formation. Hence the name "quasistationary."

[2] The wave evolves slowly it its amplitude, phase velocity, and profile do not change very much during one period of oscillation of the trapped particles.

[1] A. I. Akhelzer and G. Ya. Lyubarskiĭ, Dokl. Akad. Nauk SSSR 80, 193 (1951).

[2] A. I. Akhiezer, I. Z. Akhiezer, R. V. Polovin, A. G. Sitenko, and K. N. Stepanov, Élektrodinamika plazmy (Plasma Electrodynamics), Nauka, 1974.

[3] G. M. Zaslavskiĭ, Usp. Fiz. Nauk 111, 395 (1973) [Sov. Phys. Usp. 16, 761 (1974)].

[4] B. N. Rutkevich, A. V. Pashchenko, V. D. Fedorchenko, and V. I. Muratov, Zh. Tekh. Fiz. 42, 493 (1972) [Sov. Phys. Tekh. Phys. 17, 391 (1972)].

[5] H. Ikezi, P. J. Barrett, R. W. White, and A. I. Wong, Phys. Fluids 14, 1997 (1971).

[6] V. D. Fedorchenko, Yu. P. Mazalov, A. S. Bakaĭ, A. V. Pashchenko, and B. N. Rutkevich, Z. Eksp. Teor. Fiz. 70, 1768 (1976) [Sov. Phys. JETP 44, 920 (1976)].

[7] D. Bohm and E. P. Gross, Phys. Rev. 75, 1851 (1949).

[8] V. D. Fedorchenko, Yu. P. Mazalov, A. S. Bakaĭ, and B. N. Rutkevich, Pis'ma Zh. Eksp. Teor. Fiz. 20, 159 (1974) [JETP Lett. 20, 67 (1974)].

[9] I. B. Bernstein, J. M. Green, and M. D. Kruskal, Phys. Rev. 108, 546 (1957).

[10] A. S. Bakĭ, V in: Problemy teorii plazmy (Problems in Plasma Theory), Naukova Dumka, 1976, p. 248.

[11] A. S. Bakai, B in: Voprosy atomnoĭ nauki i tekhniki (Problems in Atomic Science and Technology), Fiz. Plazmy i UTS, No. 1(5), Kharkov, 1976.

[12] V. T. Astrelin and N. S. Buchel'nikova, Preprint No. 74-93, Institute of Nuclear Physics, 1974; Proc. Twelfth Intern. Conf. on Phenomena in Ionized Gases, Vol. 1, 1975, p. 283.

[13] A. S. Bakaĭ, S. S. Krivulya, V. D. Fedorchenko, and V. I. Muratov, Pis'ma Zh. Eksp. Teor. Fiz. 21, 226 (1975) [JETP Lett. 21, 101 (1975)].

[14] A. S. Bakaĭ, S. S. Krivulya, V. D. Fedorchenko, and I. N. Onishchenko, Zh. Eksp. Teor. Fiz. 72, 499 (1977) [Sov. Phys. JETP 45, 261 (1977)].

[15] A. S. Bakaĭ, S. S. Krivulya, and V. D. Fedorchenko, Pis'ma Zh. Tekh. Fiz. 3, 928 (1977) [Sov. Tech. Phys. Lett. 3, 379 (1977)].

[16] A. B. Mikhaĭlovskiĭ, Teoriya plazmennykh neustoĭchivosteĭ (Theory of Plasma Instabilities), Vol. 1, Atomizdat, 1970.

[17] V. D. Fedorchenko, Yu. P. Mazalov, and B. N. Rutkevich, Zh. Tekh. Fiz. 43, 710 (1973) [Sov. Phys. Tech. Phys. 18, 448 (1973)].

[18] V. D. Fedorchenko, B. N. Rutkevich, and V. I. Muratov, Nucl. Fusion 11, 43 (1971).

[19] V. D. Fedorchenko, Yu. P. Mazalov, A. S. Bakaĭ, and B. N. Rutkevich, Zh. Eksp. Teor. Fiz. 65, 2225 (1973) [Sov. Phys. JETP 38, 1111 (1974)].

Translated by S. Chomet